ARMY RESEARCH LABORATORY

Polymer-Layered Silicate Nanocomposites From Model Surfactants at High Coverage

by Frederick L. Beyer, Arnab Dasgupta,
and Mary E. Galvin

ARL-TR-2742 May 2002

The findings in this report are not to be construed as an official Department of the Army position unless so designated by other authorized documents.

Citation of manufacturer's or trade names does not constitute an official endorsement or approval of the use thereof.

Destroy this report when it is no longer needed. Do not return it to the originator.

Army Research Laboratory
Aberdeen Proving Ground, MD 21005-5069

ARL-TR-2742 **May 2002**

Polymer-Layered Silicate Nanocomposites From Model Surfactants at High Coverage

Frederick L. Beyer
Weapons and Materials Research Directorate, ARL

Arnab Dasgupta and Mary E. Galvin
University of Delaware

Abstract

A series of experiments has been designed and conducted to test a recent model for the morphological behavior of polymer-layered silicate (PLS) nanocomposites, where a PLS nanocomposite is comprised of a homopolymer matrix, layered silicate clay mineral filler, and an organic surfactant modifier. For nearly complete exchange of naturally occurring interlayer cations with model surfactants synthesized for this study, the effect of surfactant length on the morphology of polymer-layered silicate nanocomposites has been examined. Here the surfactant and matrix homopolymer are both based on polystyrene and are therefore expected to be miscible. Small-angle x-ray scattering data show that there was no intercalation of the homopolymer into the modified layered silicate. This finding is consistent with autophobic dewetting such as that which occurs with densely grafted polymer brushes, based on high surfactant coverage within the layered silicate galleries.

Acknowledgments

The authors wish to thank Professor Darrin Pochan for assistance with small-angle x-ray scattering (SAXS) data collection, Frederick Cox for matrix-assisted laser desorption ionization (MALDI) analysis, and Professor Anna Balazs for helpful interpretation of the theoretical aspects of this work. In addition, Mary E. Galvin gratefully acknowledges funding from the American Chemical Society (ACS) Petroleum Research Fund and the U.S. Army.

INTENTIONALLY LEFT BLANK.

Contents

INTENTIONALLY LEFT BLANK.

List of Figures

List of Tables

INTENTIONALLY LEFT BLANK.

1. Introduction

Polymer-layered silicate (PLS) nanocomposites have generated substantial interest in the materials community in the last decade, beginning with the publication of the findings from work at Toyota [1–3]. These works focused on the synthesis and physical properties of PLS nanocomposites based on nylon 6. The resulting materials exhibited substantively improved properties. Most of the subsequent work on PLS nanocomposites has also focused on using equally direct methods to produce materials with similarly improved physical properties and specific morphologies [4, 5]. While much has been learned, one fundamental aspect of the behavior of these materials that has not been elucidated is the underlying thermodynamic relationships between the components in the system, which at equilibrium determine the morphological behavior of the final nanocomposite.

PLS nanocomposites contain two basic components—a 2:1 mica-type layered silicate clay mineral and a polymer matrix. Layered silicate clay minerals are composed of individual microscopic sheets ~1 nm thick [6, 7]. The individual sheets stack together to form overall macroscopic clay particles called tactoids. In a 2:1 layered silicate the sheets have three layers: an inner layer of alumina octahedra sandwiched between outer layers of silica tetrahedra, in which isomorphous substitutions of different metals for aluminum and silicon create a net charge imbalance within the sheet. Hydrated cations present in the galleries eliminate this imbalance and through a cation exchange reaction, can be replaced with organic surfactants.

With the exception of hydrophilic polar polymers such as poly (ethylene oxide [8]), exchange of the naturally occurring cations in the silicate galleries with small-molecule organic surfactant has been found to be helpful for the formation of PLS nanocomposites. PLS nanocomposites are most often fabricated by either in situ polymerization of the matrix monomer in the presence of the modified layered silicate, solution intercalation where both the matrix polymer and clay are dispersed in a common solvent followed by precipitation, or melt processing that typically involves mechanical mixing of the matrix and filler. All three techniques limit the polymer systems from which PLS nanocomposites can be made. In situ polymerization methods affect the molecular characteristics of the polymer matrix. Solution processing requires the availability of a cosolvent for the hydrophilic clay and the often hydrophobic polymer. Mechanical processing places limitations on the stability and physical properties of the polymer matrix and can adversely affect the silicate clay layers. Additionally, these processes do not produce materials definitively at their thermodynamic equilibrium. The only remaining fabrication technique, direct melt intercalation [8–10], is difficult and

often unproductive. As a result, little information is available about the underlying thermodynamic relationships between layered silicate, surfactant, and matrix polymer. Understanding these relationships should allow the fabrication of PLS nanocomposites from materials chosen for their specific properties rather than formation of PLS nanocomposites from only materials that are conducive to one of these three techniques.

Recent work by Balazs, Singh, and Zhulina has provided a theoretical framework for probing the behavior of these materials in terms of the physical characteristics of the constituent materials [11]. The model calculates free energy as a function of the spacing between two surfaces representing sheets of layered silicate clay mineral. It incorporates the areal density of a surfactant on the silicate surface, or coverage, given as ρ (chains/lattice unit), the length of the surfactant, N_{gr}, and the length of intercalating homopolymer, N. Enthalpic interactions are given in terms of separate χ values, where χ is a Flory-Huggins-type interaction parameter. The parameter for surfactant and polymer is given as χ for silicate surface and surfactant, χ_{ssurf}, and for silicate surface and polymer, χ_{surf}. The model predicts a broad range of morphological behaviors depending on the enthalpic interactions between polymer and surfactant. A second result predicted is that the length of surfactant should influence the morphological behavior by affecting the degree to which the entropic penalty to an intercalating homopolymer is reduced; lengthening the surfactant should facilitate intercalation by providing a greater reduction in the entropy penalty to the intercalating homopolymer.

In this work, a series of model PLS nanocomposite samples were fabricated and characterized to investigate the effect of surfactant length on nanocomposite morphology for the simplest case probed in the Balazs model. In that case, the surfactant and homopolymer have neither attractive nor repulsive enthalpic interactions ($\chi = 0$). The layered silicate montmorillonite was modified with a series of polystyrene (PS)-based surfactants spanning a wide range in molecular weight. Unlike most recent work with PS nanocomposites, where solution and in situ polymerization fabrication techniques have been used to fabricate the PS nanocomposites [12–15], direct melt intercalation of a polymer melt was used to avoid formation of non-equilibrium structures. The modified clays were mixed with PS homopolymers, then annealed for a period of time estimated to allow the samples to approach equilibrium. The molecular weights of the surfactants and PS homopolymer were chosen for direct comparison to the Balazs model. The resulting composites were then characterized to determine if there was any morphology effect correlated with the surfactant molecular weight.

2. Experimental

Na-montmorillonite (SWy-2) layered silicate was obtained from the Missouri Clay Repository. Impurities were removed by dispersing the clay in deionized water and then centrifuging. The remaining clean clay mineral was dried, then ground with a mortar and pestle into a powder. The cation exchange capacity (CEC) of the clay was given as 76.4 meq/100 g. The measurement technique and conditions by which CEC was determined are not specified. Montmorillonite has an internal surface area of ~750 m^2/g, and a total surface area of 800 m^2/g [16]. For calculations of coverage, the more conservative total area was used.

PS was chosen as the basis of both the surfactant and matrix materials. This eliminated attractive and repulsive enthalpic interactions between the surfactant and polymer, where by definition $\chi = 0$. Amine-terminated PS surfactants were prepared following a method developed by Quirk and Lee [17]. Amine end functionalization could be achieved in nearly quantitative yield. A peak at δ = 67.9 ppm in the ^{13}C-NMR spectra of the samples scanned in acetone-d_6 confirmed the presence of the $-N(CH_3)_2$ carbons in the polymer. TLC in a mixture of ethyl acetate and hexane (3:7, v/v) was done to detect presence of unfunctionalized polystyrene in the samples. Amine-terminated PS could be separated from the unfunctionalized fraction by column chromatography using the same solvent mixture as an eluent. The amine-functionalized polymers were then quaternized quantitatively by refluxing overnight with an excess of dimethylsulphate in dry tetrahydrofuran (THF) and precipitated from a concentrated solution in methanol. In the molecular weight range of the samples studied, all amine-functionalized polymers show significant elution behavior in THF, while the quaternized samples do not elute at all. TLC of the dimethylsulphate-treated products in THF showed that the spot did not climb (elute) at all confirming absence of any amine-terminated PS in the samples. Quaternary ammonium $[-(CH_3)_3N^+]$ end functionalized PS surfactants with number averaged molecular weights of 17,600, 11,200, 6800, 2700, and 1735 g/mol were thus prepared. Molecular weights and molecular weight distributions were obtained from gel permeation chromatography (GPC) of the amine-functionalized PS samples. Analyses were performed using THF as the solvent eluting at a flow rate of 1 mL/min through two PL gel 5-μ mixed-D columns connected in series and equipped with a Hewlett-Packard (HP) 1047A refractive index (RI) detector. For the sample having a molecular weight of 1735 g/mol, matrix-assisted laser desorption ionization (MALDI) spectra were obtained in a Bruker biflex-III instrument operating in reflector mode.

A goal of complete cation exchange of the PS-based surfactant with the naturally occurring interlayer cations was selected for simplicity. This is consistent with many commercially available modified layered silicates, although generally the surfactant in those materials are short-chain alkyl quaternary amines. Complete surfactant exchange was also hoped to minimize interactions between the hydrophobic homopolymer and hydrophilic clay sheets. The modification of montmorillonite with the quaternary amine-terminated PS surfactants was carried out by treating a dispersion of the clay in a 3:1 (v/v) mixture of water and either acetone or THF, with a solution of the surfactant in the same solvent used for clay dispersion. The surfactant solution was introduced all at once into the clay dispersion, resulting in the immediate formation of a white precipitate. The precipitate was filtered and washed several times with THF to remove any unbound PS and was dried under vacuum overnight at 105 °C to remove residual solvent and water before x-ray characterization. Five surfactant molecular weights were ultimately examined, ranging from a short surfactant ~16 repeat units long to a polymeric surfactant ~167 repeat units long.

Surfactant content and coverage of the silicate surfaces was determined from thermogravimetric analysis (TGA) of the modified clays using a TA Instruments Hi-Res TGA 2950. A small amount of each modified clay was heated from room temperature through 650 °C at a rate of 10 °C/min. The residue at 650 °C was taken as the clay content, and the weight loss was used to determine surfactant coverage.

The PLS nanocomposites were fabricated by manually mixing the modified clay with a low polydispersity (PDI ≤ 1.06), 10,000 g/mol, PS standard from Pressure Chemical Company. No solvent was used in this process. In a small vial, a specific amount of modified clay was added to a specific amount of the commercial PS homopolymer. The weight of modified clay added to a given weight of PS homopolymer was adjusted so that in each sample, the weight of the montmorillonite clay mineral was ~5% of the total sample weight. These physical mixtures were pressed into pellets with contact pressure, annealed under vacuum for 1 week at 125 °C, and cooled under vacuum to room temperature. An estimate of the time it might take a PS homopolymer of 10,000 g/mol molecular weight to self-diffuse over a distance of 0.5 μm, half the lateral dimension of a large clay tactoid, was taken as a guide to the minimum annealing time necessary. Based on work done in the Rouse regime, diffusion coefficient of a 10,000 g/mol PS chain in a matrix of 10,000 g/mol PS was calculated to be 3×10^{-14} cm^2/s [18]. Using the Einstein rule, a diffusion time of ~24 hr (at 116 °C) is calculated for 0.5 μm. This estimate is conservative for three reasons: (1) A Rouse model of chain dynamics fit the data used while in the current work—Zimm behavior is expected since 10,000 g/mol is well below the entanglement molecular weight of PS [18–20]; (2) The annealing temperature in this experiment is slightly higher at 125 °C than in reference [18]; and (3) The

average particle size of Wyoming montmorillonite is likely much less than 1 μm in diameter. Balancing a concern for adequate annealing time was the possibility of degradation of the samples if left at elevated temperatures for too long. Therefore, an annealing period of 1 week, at 125 °C was used in this work.

Small-angle x-ray scattering (SAXS) and transmission electron microscopy (TEM) were used to characterize morphology. Most SAXS data were collected at the National Synchrotron Light Source at the Brookhaven National Laboratories, Upton, NY. Data were collected at a camera length of 208 cm and a wavelength of 1.605 Å, using a Bruker AXS 2D CCD detector. Data for the unmodified montmorillonite were collected using a Siemens D5005 powder diffractometer, using Cu-K_α radiation. Two-dimensional (2-D) data were corrected for detector dark current, detector sensitivity, and background scattering where Kapton film was used to support the sample. The isotropic 2-D data sets were then circularly averaged for examination of intensity as a function of scattering angle. No correction was made for differing absorptions based on varying clay content. TEM was completed using a JEOL 200CX operated at 200-kV accelerating voltage. Microtomed sections were prepared using a Leica FCS Ultracut microtome and a Microstar diamond knife.

3. Results and Discussion

The sample nomenclature used in this work describes the salient molecular characteristics of the surfactants and homopolymers used in each sample. Each sample is described with a label such as M-A-B, where "M" indicates that montmorillonite was the clay mineral, "A" is the approximate molecular weight of the surfactant modifier in kilograms per mole, and "B" is the approximate molecular weight of the PS homopolymer matrix, in kilograms per mole. For example, sample M-2-10 is composed of montmorillonite modified with the 1735 g/mol surfactant, which is contained in a matrix of PS homopolymer 10,000 g/mol in molecular weight. Sample M-2 refers to the modified montmorillonite alone, with no homopolymer matrix.

Table 1 describes the molecular characteristics of the surfactants synthesized for this experiment. The polydispersity index (PDI) is given as M_w/M_n. As a result of the living anionic nature of the polymerization of the base polystyrene oligomer or polymer, the polydispersities of the oligomers, polymers, and the surfactant end product after quaternization are quite low.

Table 1. Surfactant molecular characteristics.

Surfactant	M_n (g/mol)	M_w (g/mol)	PDI
QPSt-16	1735	1820	1.05
QPSt-15	2700	2800	1.04
QPSt-14	6800	7000	1.03
QPSt-19	11200	11600	1.04
QPSt-20	17600	18100	1.03

Table 2 lists the molecular and morphological characteristics of the modified clays. Weight-percent clay was determined using TGA, and from that measure, coverage and area/cation were calculated. With the exception of modified clay M-18, all coverages were in excess of 75%, with an average area per cation ranging from 1.9 to 3.2 nm^2/cation. Such coverages are similar to those found in commercially available short-chain alkyl-modified silicate fillers.

Table 2. Characterization data for modified clays.

Sample	Surfactant	Weight-Percent Clay	Coverage (%)	Area/Cation (nm^2)	q^* ($Å^{-1}$)	Standard Deviation ($Å^{-1}$)	d (Å)	Gallery Height (Å)
M-2	QPSt-16	49.5	76.8	2.6	0.121	0.0204	51.9	41.9
M-3	QPSt-15	38.4	77.7	2.2	0.0800	0.0145	78.5	68.5
M-7	QPSt-14	19.7	76.9	2.3	0.0488	0.00805	129	119
M-11	QPSt-19	11.4	90.9	1.9	0.0476	0.00927	132	122
M-18	QPSt-20	12.1	54.2	3.2	0.0406	0.00659	155	145

Table 3 gives the composition of the PLS nanocomposites fabricated using modified clays and PS homopolymer. The weight of modified clay and weight of homopolymer in the sample were recorded at the time the samples were fabricated. The weight of clay mineral was calculated using TGA data for composition and the weight of modified clay in each sample. The total weight percentage of clay mineral is based on the total weight and the weight of the clay mineral in each sample.

Table 3. Composition and morphological characterization data for PLS nanocomposites based on model PS-based surfactants and 10,000 g/mol PS homopolymer.

Sample	Weight Clay (g)	Weight Modified Clay (g)	Weight PS Homopolymer (g)	Weight-Percent Clay	q^* ($Å^{-1}$)	Standard Deviation ($Å^{-1}$)	d (Å)	Gallery Height (Å)
M-2-10	0.013	0.024	0.243	4.7	0.122	0.0180	51.5	41.5
M-3-10	0.014	0.036	0.253	4.7	0.0809	0.0135	77.7	67.7
M-7-10	0.0080	0.041	0.125	4.8	0.0487	0.00852	129	119
M-11-10	0.014	0.121	0.156	5.2	0.0472	0.00837	133	123
M-18-10	0.014	0.143	0.150	5.1	0.0408	0.00869	154	144

Figure 1 shows a TEM micrograph collected from modified clay sample M-7, showing clearly the separation of silicate layers resulting from modification of the clay surfaces with PS-based surfactant. TEM data were not collected for all the modified clays due to the consistency of SAXS data shown in Figures 2 and 3.

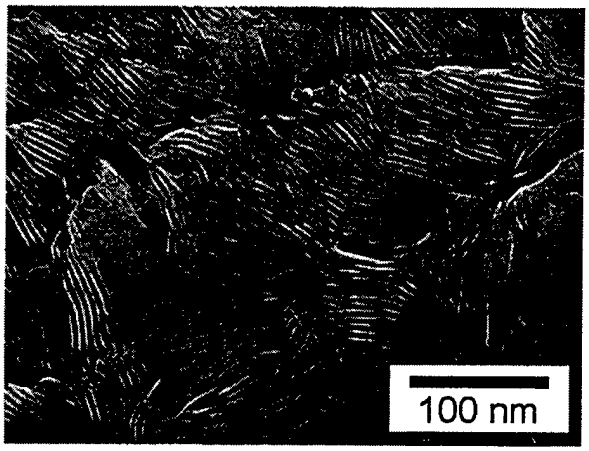

Figure 1. Representative TEM micrograph showing the separation of silicate layers after modification with PS-based surfactant, sample M-7. No PS homopolymer is present in this sample.

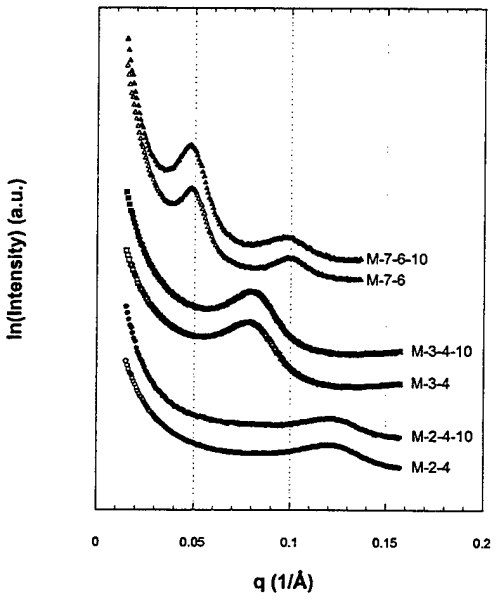

Figure 2. SAXS data for modified clays alone and nanocomposites after annealing, showing negligible change in Bragg peak locations. The unchanged peak locations reveal no intercalation of the PS homopolymer into the PS-surfactant modified montmorillonite.

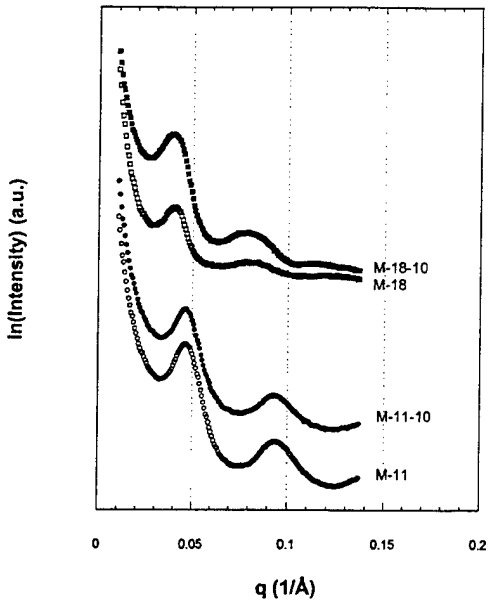

Figure 3. SAXS data for modified clays before and after annealing with PS homopolymer for the two longest surfactants.

Figure 2 shows SAXS data collected for the modified clays and PLS-nanocomposites M-2, M-2-10, M-3, M-3-10, M-7, and M-7-10. Figure 3 shows the SAXS data collected for the modified clays and PLS-nanocomposites M-11, M-11-10, M-18, and M-18-10. In both cases, the intensity data have been scaled for convenience of having several sets of data in each graph and are given as ln(I); thus, the intensity units are arbitrary and not to scale. A Gaussian probability function with a sloping linear background was fit to the primary Bragg reflection. The spacing of the first order Bragg reflection, q^*, was taken as the mean of the Gaussian peak. The standard deviation is reported as a measure of the breadth of the first order reflection. Tables 2 and 3 list q^*, standard deviation, the corresponding real space length d, where $d = 2\pi/q^*$, and gallery height (d – 10Å) for the modified clays and PLS nanocomposites, respectively.

The intent of this work was to examine the effect on equilibrium morphological behavior of the relationship between surfactant length and intercalating homopolymer in a system in which the enthalpic interactions between surfactant and homopolymer are minimal. Specifically, when $\chi = 0$, does lengthening the surfactant affect the morphological behavior of this PLS nanocomposite?

The SAXS data shown in Figures 2 and 3 reveal the morphological behavior of the PLS nanocomposites fabricated for this work. For each modified clay, the location of the primary Bragg reflection (given in Table 2) is shifted to lower q than for unmodified clay, which when dry has a periodicity of ~10 Å. This indicates the success of the cation exchange procedure. This modification is

confirmed by TGA data that allow calculation of coverage based on the cation exchange capacity and molecular weight of the surfactant modifier. Very high exchanges and coverages were achieved for each surfactant.

More important, however, is the lack of change in SAXS data between each modified clay sample and the corresponding PLS nanocomposite. The SAXS data reflect the morphology of each sample unambiguously. For a sample where intercalation occurs, the SAXS data should show a shift to lower q of the primary Bragg reflection, relative to q^* for the modified clay only. Higher-order Bragg reflections would also be shifted for intercalation. For exfoliation, the SAXS data should show basically no Bragg reflections and only a peak representing a mean correlation length between individual dispersed silicate layers. However, the samples characterized in this work show essentially no change in the SAXS data, consistent with no change in the structure of the feature giving rise to x-ray contrast, the silicate layers. Therefore, no intercalation is occurring in these materials, and only phase-separated morphologies are formed.

Comparison of these data with the Balazs model indicates two possible explanations for the phase-separated morphologies observed. The Balazs model predicts that for a certain surfactant coverage across the silicate surface, ignoring unfavorable enthalpic interactions between silicate and intercalating homopolymer, various behaviors of free energy as a function of gallery height can be expected for differing enthalpic interactions (χ) between surfactant and homopolymer. Specifically, for $\chi = 0$, with a surfactant 25 units long, a polymer 100 units long, and a surface density of $\rho = 0.04$ chains/lattice site, the Balazs model predicts that an intercalated morphology will be formed. These conditions are met by sample M-3-10, with the exception of coverage. The Balazs model is a mean-field model with a lattice having a dimension equal to that of the Kuhn length of the polymer in question. For a PS-based system, $\rho = 0.04$ (chains/lattice area unit) corresponds to an area of $25 \cdot (0.69\ \text{nm})^2$, or 11.9 nm^2/surfactant [21]. In the case of sample M-3, the area/cation is calculated to be ~2.2 nm^2, which corresponds to $\rho = 0.22$. Thus, it is clear that in regard to coverage, the modified clays fabricated for this work fall outside the range considered in the Balazs model predictions.

Additionally, Balazs et al. [11] examined the effect of surfactant coverage on the free energy potential as a function of gallery height and thus equilibrium morphological behavior. For $\chi = 0$, a surfactant 25 units in length, a homopolymer 100 units in length, and a surface coverage of $\rho = 0.12$ or 4.0 nm^2/surfactant, they found the free energy potential in this case was shifted significantly toward behavior indicative of phase separation; for all gallery heights, the change in free energy was less, and the minimum was shallower. It is reasonable to expect that at coverages comparable to those for these samples ($\rho = 0.22$), the Balazs model would predict phase separation.

Finally, the phase separation of the modified clays from the PS matrix is consistent with autophobic behavior previously observed in polymer brush systems, such as flocculation of surfactant-coated colloidal particles [22], and described well theoretically [23, 24]. In the nomenclature of these works, a polymer brush is densely grafted if $\sigma\sqrt{N} > (N/P)^2$, where σ is the grafting density, N is the degree of polymerization of the grafted brush, and P is the degree of polymerization of the polymer melt. Table 4 gives these values for the modified clays in this work and also for the conditions used in the Balazs model, where surfactant density is $\rho = 0.04$, the surfactant is 25 units long, and the polymer melt is 100 units long. Because the relationship above is a scaling relationship, it is most convenient to examine $f(\sigma;N,P) = (\sigma\sqrt{N})/(N/P)^2$, which should be greater than some constant. For the purposes of this work, it is sufficient to note whether a modified clay has a more densely grafted brush than the hypothetical modified clay considered in the Balazs model. Therefore, Table 4 lists f calculated for each modified clay made for this work, normalized by a value f_B. Here, f_B is the value of f calculated for the hypothetical sample conditions used by Balazs et al. [11]. In this manner, a sample that has a brush more dense than that in the Balazs model (f_B), will be indicated by a value of $f/f_B > 1$.

Table 4. Calculations for comparison of coverage data with behavior predictions from autophobic dewetting theory.

Sample	σ (nm^{-2})	N	$\sigma\sqrt{N}$	$(N/P)^2$	f	f/fB
Balazs Model	0.084	25	0.42	0.063	6.7	1.0
M-2-10	0.38	16	1.5	0.030	51	7.6
M-3-10	0.45	25	2.3	0.073	31	4.6
M-7-10	0.43	64	3.4	0.46	7.5	1.1
M-11-10	0.53	106	5.5	1.3	4.2	0.63
M-18-10	0.31	167	4.0	3.1	1.3	0.19

One finds that, except for the two longest surfactants, which are essentially equal to or longer than the matrix homopolymer, f/f_B is greater than unity. In those samples, M-2, M-3, and M-7, and corresponding PLS nanocomposites, the density of the surfactant is at a minimum greater than that used in the Balazs model and in the case of the shortest surfactants, significantly so. Under these conditions, one would anticipate the existence of a net attractive force between particles (silicate layers), which would encourage them to flocculate. In the case of surfactant-modified layered silicates, this corresponds to phase separation with the homopolymer matrix (or a lack of deflocculation). Phase separation allows the best interaction between adjacent polymer brushes, or modified silicate surfaces.

The steadily decreasing value of normalized f/f_B also seems to reflect the prediction of the Balazs model that a longer brush can facilitate better interaction

between surfactants and the polymer matrix. That sample M-18-10 gives f/f_B, but still forms a phase separated morphology, indicating that even $f/f_B < 0.19$ may include brushes of sufficient density to cause autophobic dewetting. This result may also be due to the lower coverage of M-18-10 in comparison to the other modified clays, allowing increased interaction between the hydrophilic silicate surface and the hydrophobic PS matrix, a condition not expressly examined by Balazs et al. [11].

A final consideration in the specific parameters used in the model and the applicability of the model parameters to a real system. One interaction not specifically taken into account is the silicate surface-surfactant interaction, included in the model as χ_{ssurf}. The strongly hydrophilic surface of the clay layers and the hydrophobic PS surfactants would be expected to repel one another. This interaction is not considered in the specific predictions of the model for the hypothetical nanocomposite, as χ_{ssurf} is set to zero. Another example that would be more relevant at low coverages is the interactions between the silicate surface and the intercalating homopolymer, also a factor incorporated into the model, but not specifically investigated in the cited works.

4. Conclusions

A systematic investigation of surfactant length on the equilibrium morphological behavior in a model polymer-layered silicate nanocomposite system was conducted. PS-based surfactants were synthesized at five different molecular weights and with low polydispersity, were quaternized with a trimethylamino endgroup and exchanged with the naturally occurring cations present in the layered silicate galleries. The modified clays were then combined with PS homopolymer and annealed to allow direct melt intercalation to occur if energetically favorable, unlike most other work with PS-based nanocomposites where solution or in situ polymerization fabrication techniques are used. At high levels of surfactant coverage of the layered silicate clay mineral surfaces, no intercalation of the modified clay minerals was observed using SAXS; only phase separated morphologies were found. This behavior was found to be consistent with the predictions of the Balazs model and also with the general phenomenon of autophobic dewetting.

INTENTIONALLY LEFT BLANK.

5. References

1. Giannelis, E. P. "Polymer Layered Silicate Nanocomposites." *Advanced Materials*, vol. 8, p. 29, 1996.
2. Kojima, Y., A. Usuki, M. Kawasumi, A. Okada, Y. Fukushima, T. Kurauchi, and O. Kamigaito. "Mechanical-Properties of Nylon 6-Clay Hybrid." *Journal of Materials Research*, vol. 8, p. 1185, 1993.
3. Usuki, A., Y. Kojima, M. Kawasumi, A. Okada, Y. Fukushima, T. Kurauchi, and O. Kamigaito. "Synthesis of Nylon 6-Clay Hybrid." *Journal of Materials Research*, vol. 8, p. 1179, 1993.
4. Alexandre, M., and P. Dubois. "Polymer-Layered Silicate Nanocomposites: Preparation, Properties, and Uses of a New Class of Materials." *Materials Science & Engineering R-Reports*, vol. 28, p. 1, 2000.
5. Biswas, M., and S. S. Ray. "Recent Progress in Synthesis and Evaluation of Polymer-Montmorillonite Nanocomposites." *Advances in Polymer Science*, vol. 155, p. 167, 2001.
6. Grim, R. E. *Clay Mineralogy*. New York: McGraw-Hill, Inc., 1968.
7. Brindley, G. W., and G. Brown. *Crystal Structures of Clay Minerals and Their X-ray Identification*. London: Mineralogical Society, 1980.
8. Vaia, R. A., S. Vasudevan, W. Krawiec, L. G. Scanlon, and E. P. Giannelis. "New Polymer Electrolyte Nanocomposites—Melt Intercalation of Poly (Ethylene Oxide) in Mica-Type Silicates." *Advanced Materials*, vol. 7, p. 154, 1995.
9. Vaia, R. A., H. Ishii, and E. P. Giannelis. "Synthesis and Properties of 2-Dimensional Nanostructures by Direct Intercalation of Polymer Melts in Layered Silicates." *Chemistry of Materials*, vol. 5, p. 1694, 1993.
10. Sikka, M., L. N. Cerini, S. S. Ghosh, and K. I Winey. "Melt Intercalation of PS in Layered Silicates." *Journal of Polymer Science, Part B: Polymer Physics*, vol. 34, p. 1443, 1996.
11. Balazs, A. C., C. Singh, and E. Zhulina. "Modeling the Interactions Between Polymers and Clay Surfaces Through Self-Consistent Field Theory." *Macromolecules*, vol. 31, p. 8370, 1998.
12. Noh, M. W., and D. C. Lee. "Synthesis and Characterization of PS-Clay Nanocomposite by Emulsion Polymerization." *Polymer Bulletin*, vol. 42, p. 619, 1999.

13. Chen, G. H., D. J. Wu, W. G. Weng, B. He, and W. I Yan. "Preparation of Polystyrene-Graphite Conducting Nanocomposites via Intercalation Polymerization." *Polymer International,* vol. 50, p. 980, 2001.

14. Tseng, C. R., J. Y. Wu, H. Y. Lee, and F. C. Chang. "Preparation and Crystallization Behavior of Syndiotactic Polystyrene-Clay Nanocomposites." *Polymer,* vol. 42, p. 10063, 2001.

15. Ko, M. B., and J. Y. Jho. "Ion Exchange Reaction in Preparation of Clay-Dispersed Polystyrene Nanocomposite by Emulsion Polymerization-Coagulation Technique." *Polymer Bulletin,* vol. 46, p. 315, 2001.

16. Van Olphen, H., and J. J. Fripiat. *Data Handbook for Clay Materials and Other Non-Metallic Minerals.* New York: Pergamon Press, p. 346, 1979.

17. Quirk, R. P., and Y. Lee. "Quantitative Amine Functionalization of Polymeric Organolithium Compounds With 3-Dimethylaminopropyl Chloride in the Presence of Lithium Chloride." *Journal of Polymer Science, Part A: Polymer Chemistry,* vol. 38, p. 145, 2000.

18. Green, P. F., and E. J. Kramer. "Matrix Effects on the Diffusion of Long Polymer-Chains." *Macromolecules,* vol. 19, p. 1108, 1986.

19. Ferry, J. D. *Viscoelastic Properties of Polymers.* 3rd ed., New York: Wiley, 1980.

20. Lomellini, P. "Effect of Chain Length on the Network Modulus and Entanglement." *Polymer,* vol. 33, p. 1255, 1992.

21. Wignall, G. D. *Encyclopedia of Polymer Science and Engineering.* 2nd ed., New York: Wiley, edited by M. Grayson and T. I. Kroschwitz, p. 112, 1987.

22. Hasegawa, R., Y. Aoki, and M. Doi. "Optimum Graft Density for Dispersing Particles in Polymer Melts." *Macromolecules,* vol. 29, p. 6656, 1996.

23. Ferreira, P. G., A. Ajdari, and L. Leibler. "Scaling Law for Entropic Effects at Interface Between Grafted Layers and Polymer Melts." *Macromolecules,* vol. 31, p. 3994, 1998.

24. Shull, K. R. "Wetting Autophobicity of Polymer Melts." *Faraday Discussions,* vol. 203, 1994.

NO. OF COPIES	ORGANIZATION
2	DEFENSE TECHNICAL INFORMATION CENTER DTIC OCA 8725 JOHN J KINGMAN RD STE 0944 FT BELVOIR VA 22060-6218
1	HQDA DAMO FDT 400 ARMY PENTAGON WASHINGTON DC 20310-0460
1	OSD OUSD(A&T)/ODDR&E(R) DR R J TREW 3800 DEFENSE PENTAGON WASHINGTON DC 20301-3800
1	COMMANDING GENERAL US ARMY MATERIEL CMD AMCRDA TF 5001 EISENHOWER AVE ALEXANDRIA VA 22333-0001
1	INST FOR ADVNCD TCHNLGY THE UNIV OF TEXAS AT AUSTIN 3925 W BRAKER LN STE 400 AUSTIN TX 78759-5316
1	US MILITARY ACADEMY MATH SCI CTR EXCELLENCE MADN MATH THAYER HALL WEST POINT NY 10996-1786
1	DIRECTOR US ARMY RESEARCH LAB AMSRL D DR D SMITH 2800 POWDER MILL RD ADELPHI MD 20783-1197
1	DIRECTOR US ARMY RESEARCH LAB AMSRL CI AI R 2800 POWDER MILL RD ADELPHI MD 20783-1197

NO. OF COPIES	ORGANIZATION
3	DIRECTOR US ARMY RESEARCH LAB AMSRL CI LL 2800 POWDER MILL RD ADELPHI MD 20783-1197
3	DIRECTOR US ARMY RESEARCH LAB AMSRL CI IS T 2800 POWDER MILL RD ADELPHI MD 20783-1197
	ABERDEEN PROVING GROUND
2	DIR USARL AMSRL CI LP (BLDG 305)

NO. OF COPIES	ORGANIZATION
9	DIR USARL AMSRL WM MA F BEYER (5 CPS) A HSIEH S MCKNIGHT G SEVERE S TREVINO

REPORT DOCUMENTATION PAGE

Form Approved
OMB No. 0704-0188

1. AGENCY USE ONLY *(Leave blank)*	2. REPORT DATE	3. REPORT TYPE AND DATES COVERED
	May 2002	Interim, FY01

4. TITLE AND SUBTITLE
Polymer-Layered Silicate Nanocomposites From Model Surfactants at High Coverage

5. FUNDING NUMBERS
EMAT01

6. AUTHOR(S)
Frederick L. Beyer, Arnab Dasgupta,* and Mary E. Galvin*

7. PERFORMING ORGANIZATION NAME(S) AND ADDRESS(ES)
U.S. Army Research Laboratory
ATTN: AMSRL-WM-MA
Aberdeen Proving Ground, MD 21005-5069

8. PERFORMING ORGANIZATION REPORT NUMBER
ARL-TR-2742

9. SPONSORING/MONITORING AGENCY NAMES(S) AND ADDRESS(ES)

10.SPONSORING/MONITORING AGENCY REPORT NUMBER

11. SUPPLEMENTARY NOTES
*Department of Materials Science and Engineering, 301 Spencer Laboratory, University of Delaware, Newark, DE 19716

12a. DISTRIBUTION/AVAILABILITY STATEMENT
Approved for public release; distribution is unlimited.

12b. DISTRIBUTION CODE

13. ABSTRACT *(Maximum 200 words)*

A series of experiments has been designed and conducted to test a recent model for the morphological behavior of polymer-layered silicate (PLS) nanocomposites, where a PLS nanocomposite is comprised of a homopolymer matrix, layered silicate clay mineral filler, and an organic surfactant modifier. For nearly complete exchange of naturally occurring interlayer cations with model surfactants synthesized for this study, the effect of surfactant length on the morphology of polymer-layered silicate nanocomposites has been examined. Here the surfactant and matrix homopolymer are both based on polystyrene and are therefore expected to be miscible. Small-angle x-ray scattering data show that there was no intercalation of the homopolymer into the modified layered silicate. This finding is consistent with autophobic dewetting such as that which occurs with densely grafted polymer brushes, based on high surfactant coverage within the layered silicate galleries.

14. SUBJECT TERMS
polymer, layered silicate, montmorillonite, polystyrene, small-angle x-ray scattering

15. NUMBER OF PAGES
21

16. PRICE CODE

17. SECURITY CLASSIFICATION OF REPORT	18. SECURITY CLASSIFICATION OF THIS PAGE	19. SECURITY CLASSIFICATION OF ABSTRACT	20. LIMITATION OF ABSTRACT
UNCLASSIFIED	UNCLASSIFIED	UNCLASSIFIED	UL

INTENTIONALLY LEFT BLANK.